

### 3.3.3 Implementation of Quantum Fourier transform

$$|a\rangle \xrightarrow{F} \frac{1}{\sqrt{q}} \sum_{c=0}^{q-1} \exp\left(i \frac{2\pi ac}{q}\right) |c\rangle$$

$$|c=0\rangle = |0\rangle_1 |0\rangle_2 \cdots |0\rangle_n$$

$$|c=1\rangle = |0\rangle_1 |0\rangle_2 \cdots |1\rangle_n$$

⋮

$$|c=q-1\rangle = |1\rangle_1 |1\rangle_2 \cdots |1\rangle_n$$

$$a = a_{n-1} 2^{n-1} + a_{n-2} 2^{n-2} + \cdots + a_1 2^1 + a_0$$

$$\Rightarrow a = a_{n-1} a_{n-2} \cdots a_0$$

$$c = c_{n-1} 2^{n-1} + c_{n-2} 2^{n-2} + \cdots + c_1 2^1 + c_0$$

$$\Rightarrow c = c_{n-1} c_{n-2} \cdots c_0$$

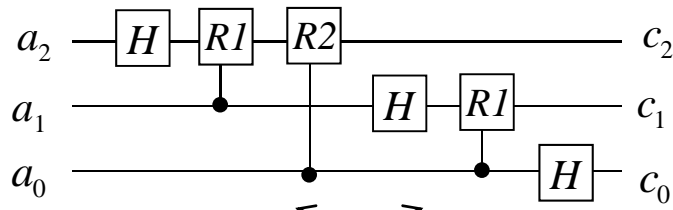
$$\frac{ac}{q} = c_{n-1} \frac{a_0}{2} + c_{n-2} \left( \frac{a_1}{2} + \frac{a_0}{2^2} \right) + \cdots + c_0 \left( \frac{a_{n-1}}{2} + \frac{a_{n-2}}{2^2} + \cdots + \frac{a_0}{2^n} \right)$$

↖  $2^n$

The terms containing  $2^m (m \geq n)$  satisfy  $e^{\frac{i 2\pi ac}{q}} = 1$ , so they can be neglected.

$$\begin{aligned} \frac{1}{\sqrt{q}} \sum_{c=0}^{q-1} e^{\frac{i 2\pi ac}{q}} |c\rangle &= \frac{1}{\sqrt{q}} \left( |0\rangle + e^{i 2\pi \frac{a_0}{2}} |1\rangle \right)_1 \otimes \left( |0\rangle + e^{i 2\pi \left( \frac{a_1}{2} + \frac{a_0}{2^2} \right)} |1\rangle \right)_2 \\ &\quad \cdots \otimes \left( |0\rangle + e^{i 2\pi \left( \frac{a_{n-1}}{2} + \frac{a_{n-2}}{2^2} + \cdots + \frac{a_0}{2^n} \right)} |1\rangle \right)_n \end{aligned}$$

example :  $n = 3$  bit

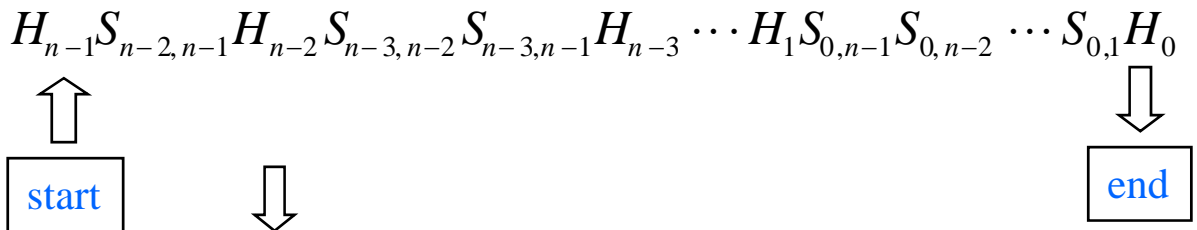


$\frac{1}{\sqrt{2}}(|0\rangle + e^{i2\pi\frac{a_0}{2}}|1\rangle)$  is produced by  $H$ .

$$\left. \begin{aligned} R_1 &= \begin{pmatrix} 1 & 0 \\ 0 & e^{i\frac{\pi}{2}} \end{pmatrix} \\ R_2 &= \begin{pmatrix} 1 & 0 \\ 0 & e^{i\frac{\pi}{4}} \end{pmatrix} \\ \vdots & \end{aligned} \right\} S_{j,k} = \begin{pmatrix} 1 & & 0 & |0\rangle_j |0\rangle_k \\ & 1 & & |0\rangle_j |1\rangle_k \\ & & 1 & |1\rangle_j |0\rangle_k \\ 0 & & & e^{i\theta_{k-j}} |1\rangle_j |1\rangle_k \end{pmatrix}$$

$\theta_{k-j} = \frac{\pi}{2^{k-j}}$

Sequence of gate operations:



$n$  WH (one-bit) gates

$$\frac{n(n-1)}{2} \Lambda_1(U) \text{ gates} \quad \leftarrow 4 \text{ one-bit gates} + 2 \text{ C-NOT gates}$$

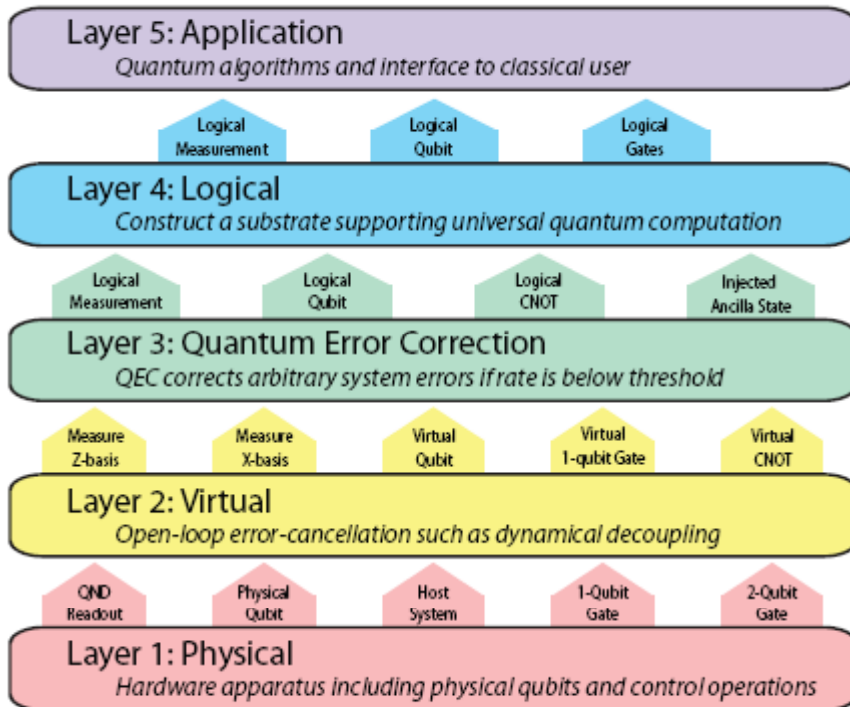
$1 + 2 + \dots + (n-1)$

$$\left. \begin{aligned} 4 \times \frac{n(n-1)}{2} + n &= 2n^2 - n \quad \text{one-bit gates} \\ 2 \times \frac{n(n-1)}{2} &= n^2 - n \quad \text{C-NOT gates} \end{aligned} \right\} \sim O(n^2)$$

### 3.4 Fault-tolerant architecture

Unfortunately, physical qubits lose their amplitude and phase information in finite lifetimes ( $T_1$ ,  $T_2$ ) due to unavoidable coupling to external worlds (reservoirs). Quantum gates always suffer from inevitable gate errors, that is, the rotation angle of a qubit cannot be controlled precisely in realistic gates. The only way to execute error-free, perfect quantum computation using erroneous quantum gates is to employ a fault-tolerant quantum computing architecture. According to the famous threshold theorem, we can correct any error introduced by the reservoir coupling and imperfect gates if and only if the gate fidelity is greater than a certain value. We will see the cost of this approach is an enormous increase in the computational resources, i.e. number of physical qubits and computational time. In this chapter, we will show the required physical resources to complete a meaningful computation are  $10^8 \sim 10^9$  physical qubits and 1 ~ 10 days of computational time.

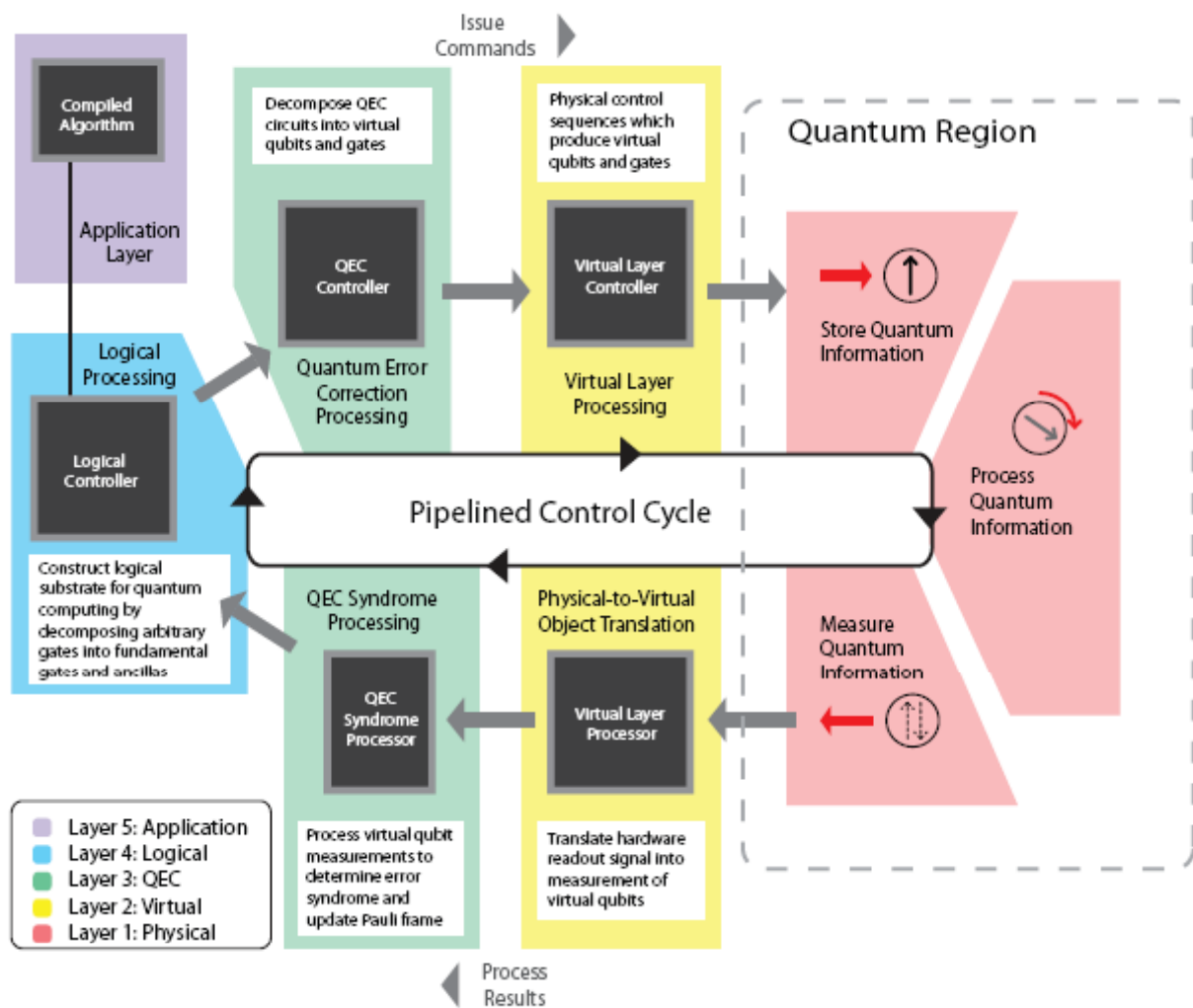
### 3.4.1 Layered architecture



Application layer: (top) A particular quantum algorithm is implemented and computational results are output to the classical user.

Physical layer: (bottom) Physical qubits and quantum gates are installed as the row physical processes.

Virtual layer: .  
 Quantum error correction layer: Shaping the faulty quantum processes in the physical layer into a sufficiently accurate system.  
 Logical layer: (intermediate)



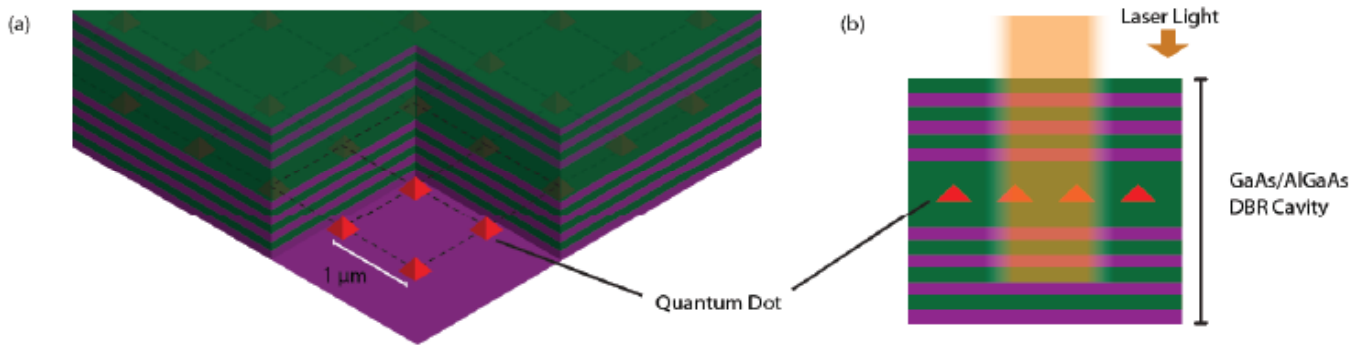
For the quantum computer to function efficiently, each layer must issue instructions to layers below in a sequence and each layer must provide results (services) to layers above simultaneously.



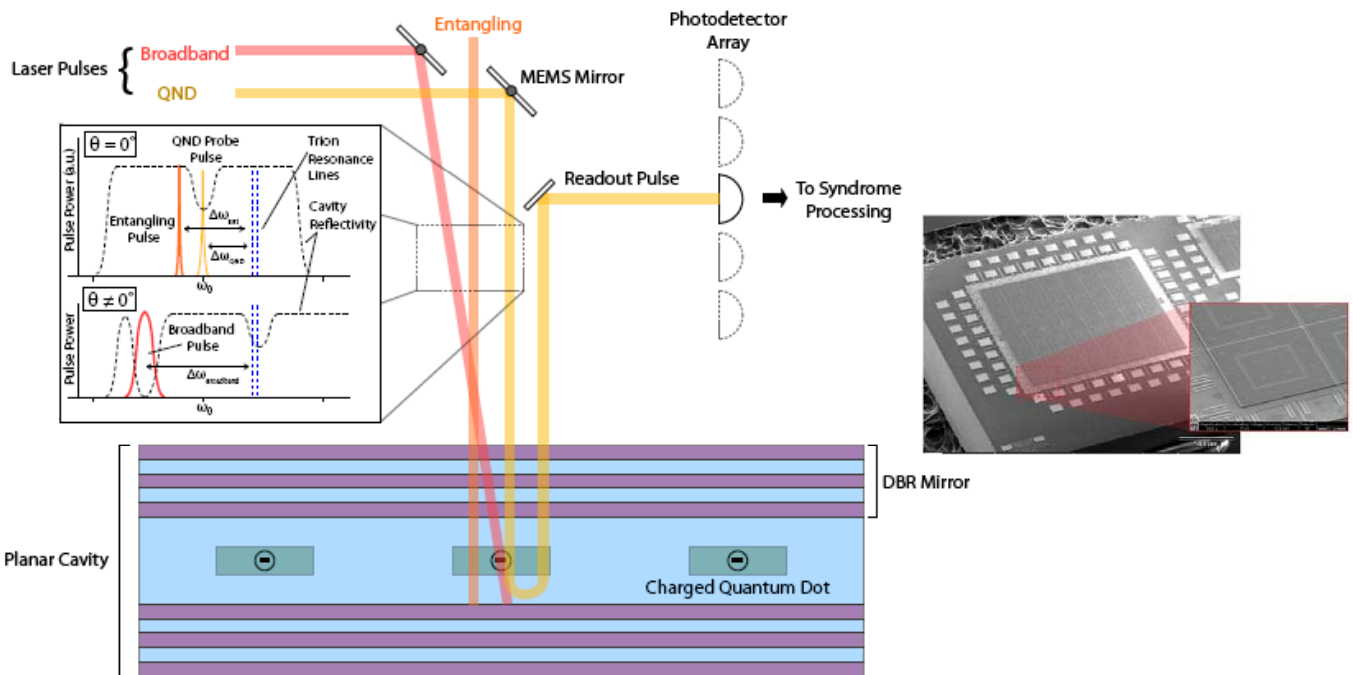
A control loop can handle those operations at all layers simultaneously, including syndrome measurement and error correction.

### 3.4.2 Physical layer

Quantum dots with optically controlled spins (QuDOS) as an example



Site controlled quantum dots with single electrons or holes are embedded in a planar microcavity.

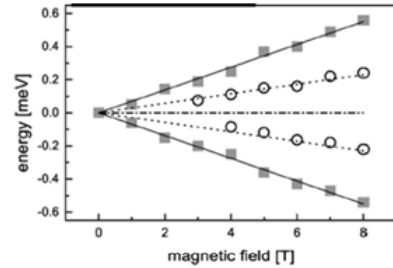
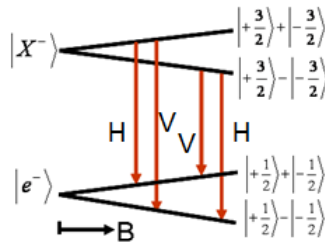
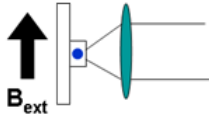


Three optical pulses, called broadband, entangling and quantum nondemolition (QND), implement the single qubit gate, two-qubit gate and projective measurement (initialization).

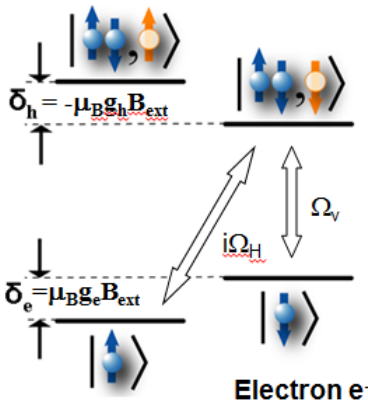
## A. Physical qubit

An electron or hole spin in quantum dots with a dc magnetic field perpendicular to the growth direction.

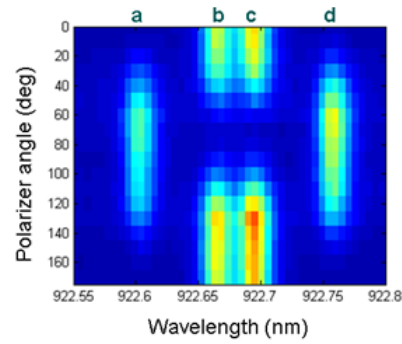
Magnetic field in Voigt geometry



Trion  $X^-$  electron spins in singlet spin is governed by heavy hole



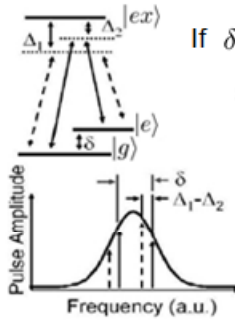
M. Bayer et al., Phys. Rev. B 65, 195305 (2002)



D. Press et al., Nature 456, 218 (2008)

## B. Single qubit gate

- A single broadband optical pulse can implement an arbitrary one-bit gate with fidelity of 0.999.



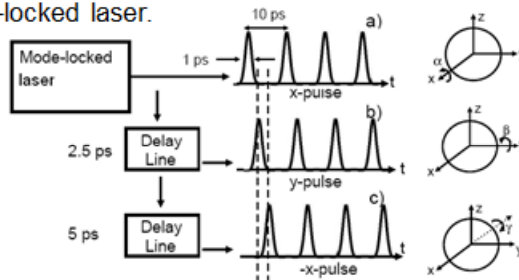
If  $\delta \ll \Omega_0, \Omega_1 \ll \Delta$ , an effective Rabi frequency

$$\Omega_{\text{eff}} = \frac{\Omega_0 \Omega_1^*}{2\Delta} \approx \frac{|\Omega(t)|^2}{2\Delta}$$

$$\Omega(t) = \frac{\mu E(t)}{\hbar}$$

rotation angle  $\int \Omega_{\text{eff}} dt$  is proportional to pulse energy

- A system clock is provided by the pulse arrival time from the mode-locked laser.



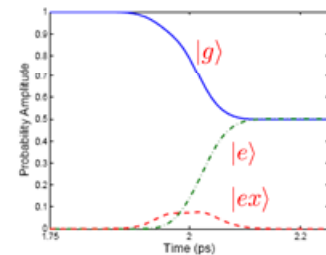
Arbitrary single qubit gates  $SU(2)$  can be implemented in one-half of Larmor oscillation period.

Experiment with an ensemble of donor spins : K.M. Fu et al., Nature Physics 4, 780 (2008)

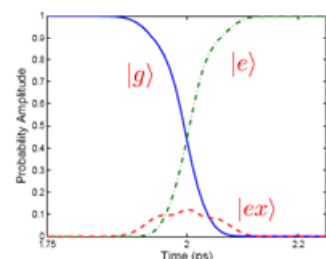
Numerical simulation based on the three-level master equation

$$\tau \ll T_1, T_2$$

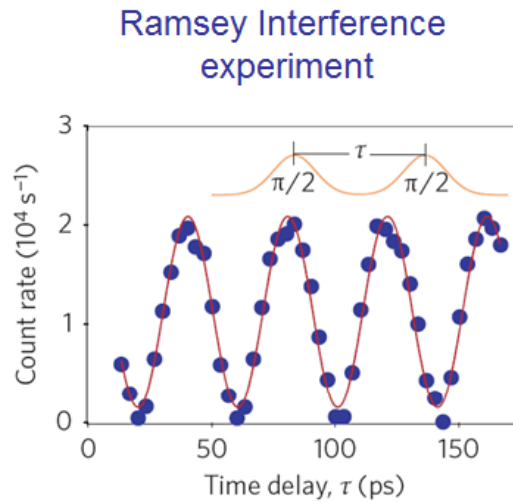
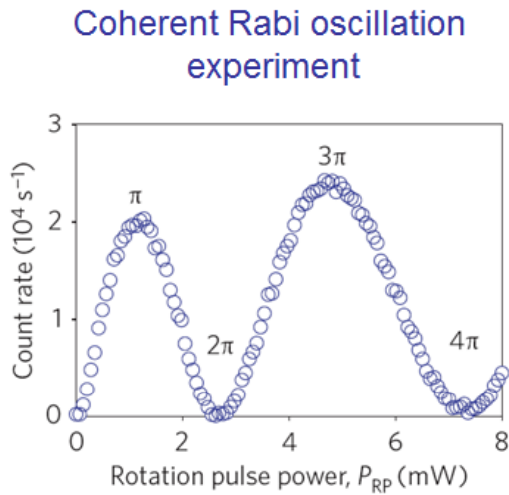
100fs  $\pi/2$  - pulse



100fs  $\pi$  - pulse



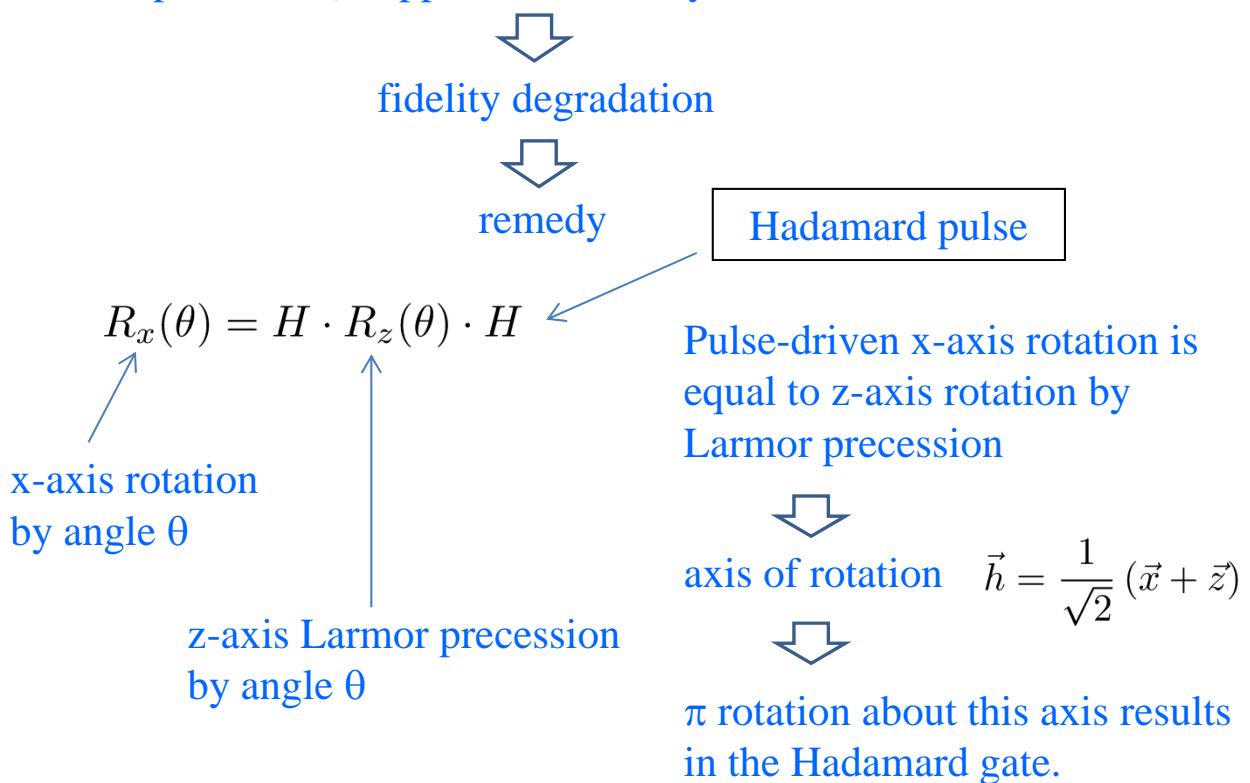
Control optical pulse energy reduced by a cavity: 1/300  
 Optical pump pulse completely off during single qubit operation

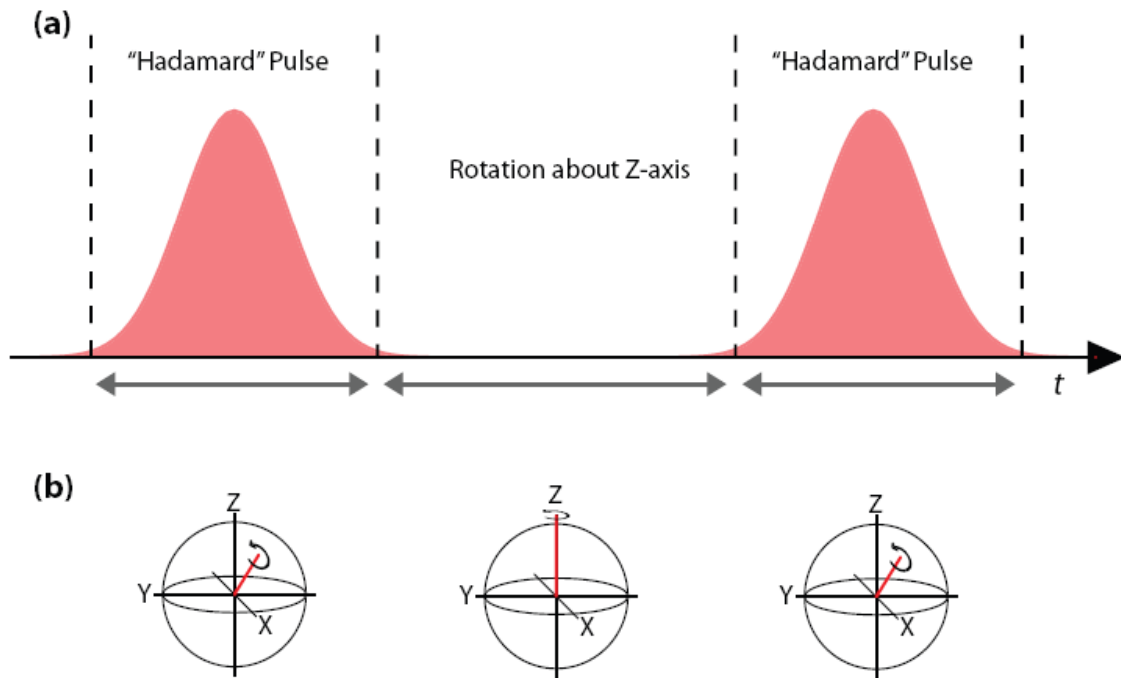


Spin rotation during control pulse  
 (Larmor period 40 psec vs. pulse duration 4 psec)

Single qubit gate fidelity:  $F=98\sim99\%$

A laser pulse has some finite duration ( $\sim 1\text{psec}$ ) which is not completely negligible compared to the Larmor precession period (10-100 psec). Thus, the rotation around x-axis (single qubit gate) and z-axis (free Larmor precession) happen concurrently.





### C. Two qubit gate

An optical pulse, whose frequency is slightly detuned from the planar cavity resonance, excites the spin dependent cavity internal field. The two spin states acquire the geometric phase after the pulse and cavity internal field are gone.

$$|\psi\rangle_i = C_0|\downarrow\downarrow\rangle + C_1|\downarrow\uparrow\rangle + C_2|\uparrow\downarrow\rangle + C_3|\uparrow\uparrow\rangle$$



$$|\psi\rangle_f = C_0e^{i\theta_0}|\downarrow\downarrow\rangle + C_1e^{i\theta_1}|\downarrow\uparrow\rangle + C_2e^{i\theta_2}|\uparrow\downarrow\rangle + C_3e^{i\theta_3}|\uparrow\uparrow\rangle$$

If  $\theta_0 = 2\pi L$

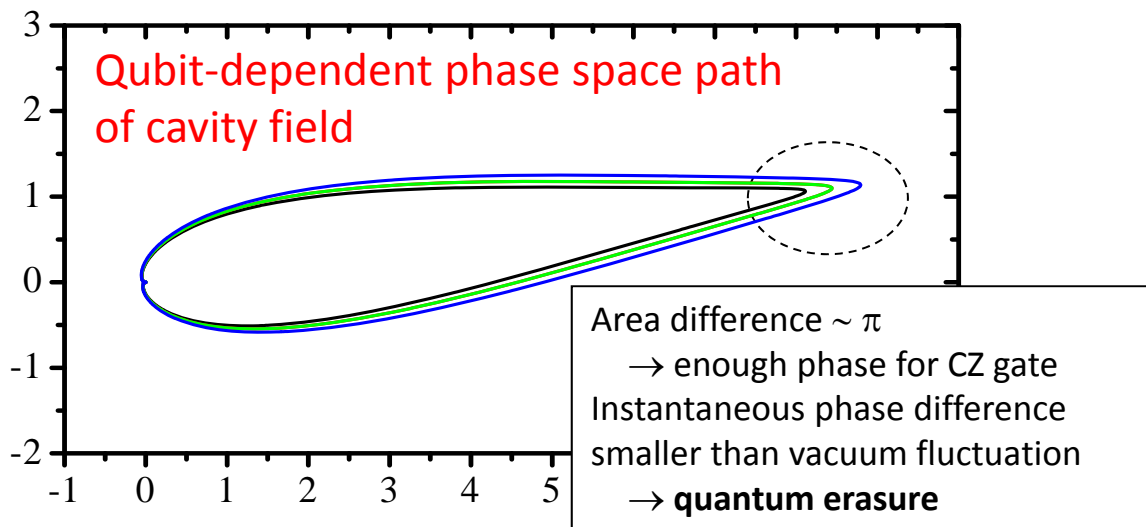
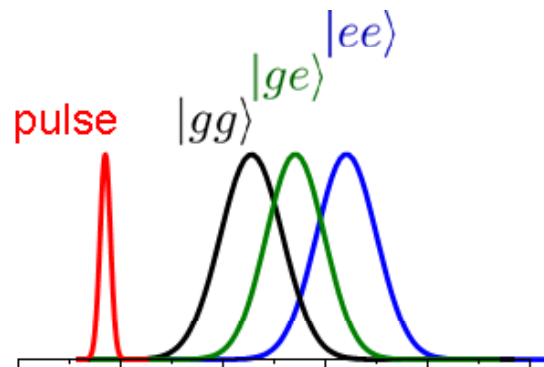
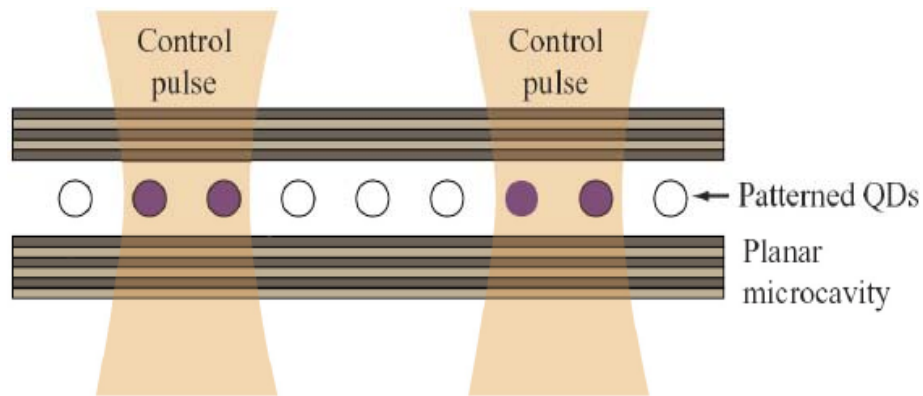
$$\theta_1 = \theta_2 = 2\pi M \quad (\text{L, M, N: positive integers})$$

$$\theta_3 = 2\pi N + \pi$$



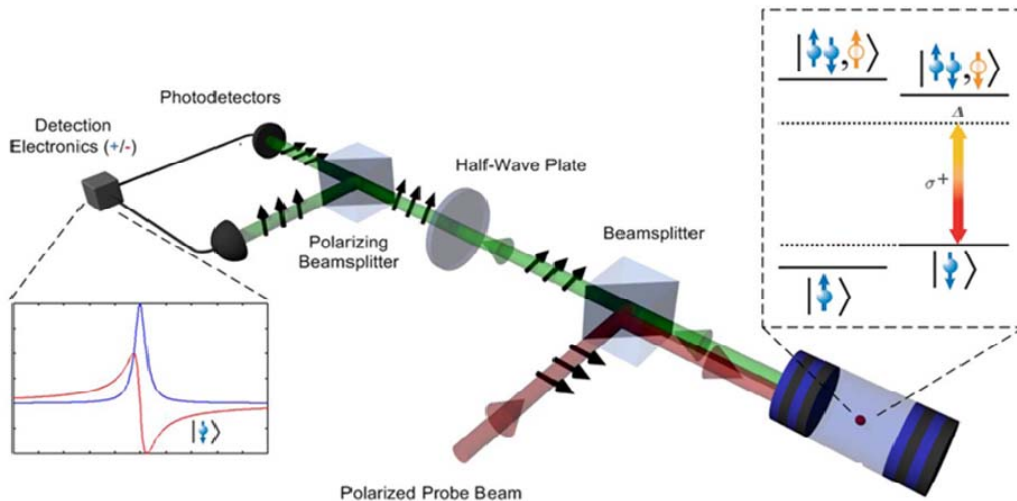
$$|\psi\rangle_f = C_0|\downarrow\downarrow\rangle + C_1|\downarrow\uparrow\rangle + C_2|\uparrow\downarrow\rangle - C_3|\uparrow\uparrow\rangle$$

This is a controlled-phase gate and can be realized by pulse duration of 10-100nsec. This gate can be implemented in a massive parallel way.



## D. Projective measurement

A planar microcavity with a single electron (hole) introduces a spin-dependent phase shift on the incident probe laser pulse. This process can be used as a means of projective measurement of a single spin and the required integration time is  $\sim 1$  nsec.



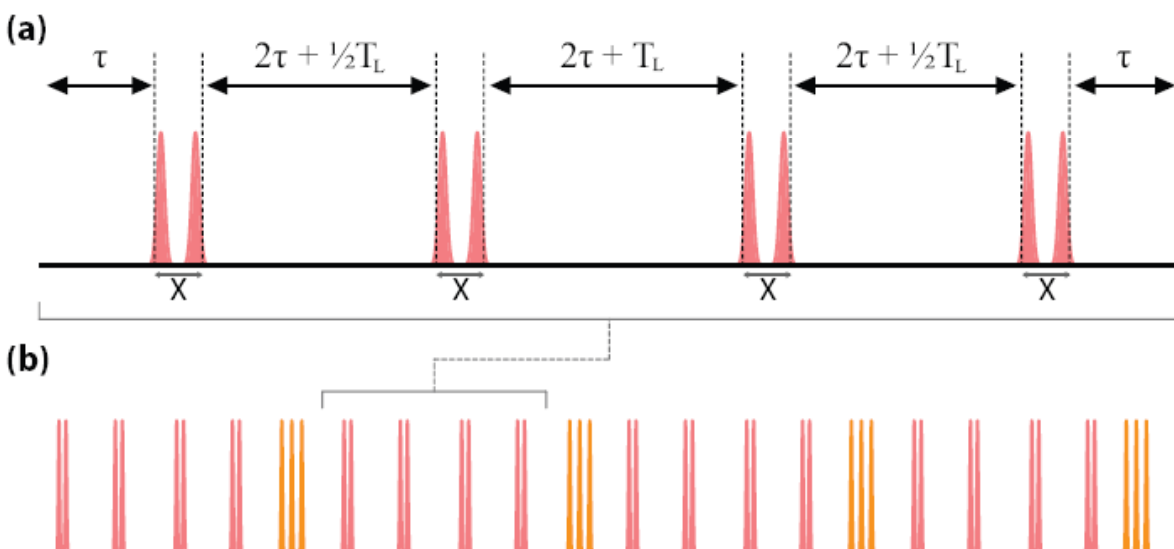
### 3.4.3 Virtual layer

Make the physical layer robust to “systematic (or correlated) errors” by enforcing symmetries in the system, i.e. canceling the errors by destructive interference.

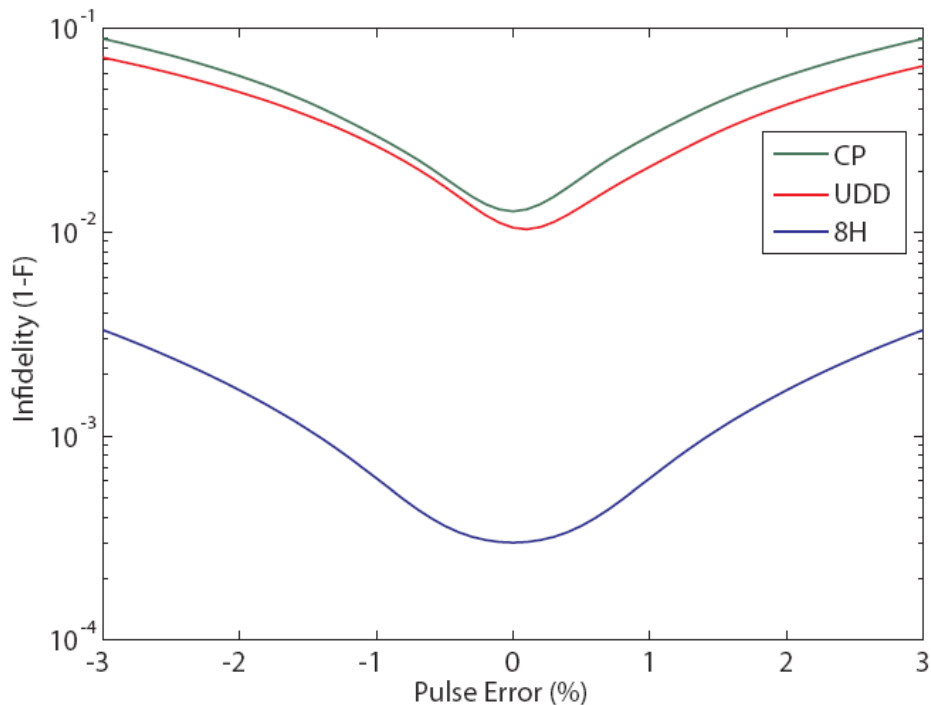
8H decoupling pulse sequence consists of eight Hadamard pulses, where  $\tau \ll T_2$  is an arbitrary time and  $T_L$  is the Larmor precession period.



It can eliminate the free evolution error (dephasing time  $T_2^*$ ) and the qubit control gate error to first-order.



- Each of the pulse pairs enacts a  $\pi$ -rotation around x-axis.
- Four pairs of 8H sequence are interleaved with arbitrary single qubit gate  $SU(2) = R_x(\alpha)R_z(\beta)R_x(\gamma)$  formed from three Hadamard pulses.
- The overall sequence forms a virtual gate by way of a BB1 compensation sequence, which requires  $\sim 32$  nsec virtual gate time.
- Measurement of virtual qubits must be performed with dynamical decoupling halted.



$$\tau = 1 \text{ nsec}$$

CP: Carr-Purcell sequence

UDD: Uhrig Dynamical Decoupling sequence



To satisfy  $1 - F < 10^{-3}$  (adequately low), control laser (energy) errors must be less than 1%.